



## $2\pi$ proportional counting chamber for large-area-coated $\beta$ sources

SHRADDHA S DESAI

Solid State Physics Division, Bhabha Atomic Research Centre, Trombay, Mumbai 400 085, India  
E-mail: ssdesai@barc.gov.in

MS received 23 December 2014; revised 15 June 2015; accepted 30 July 2015

DOI: 10.1007/s12043-016-1192-z; ePublication: 18 March 2016

**Abstract.** Detection system for measuring absolute emission rate from large-area-coated  $\beta$  sources has been indigenously developed. The system consists of a multiwire-based proportional counter with gas flow and a source mounted within the sensitive volume of the detector. Design of the counter enables efficient counting of emissions in  $2\pi$  solid angle. A provision is made for change of the source and immediate measurement of source activity. These sources are used to calibrate the efficiency of contamination monitors at radiological facilities. Sensitive area of the detector covers  $165^\circ$  solid angle nearing  $2\pi$  of emission from the source of size  $100 \times 150$  mm. Performance of the chamber is tested using collimated  $^{55}\text{Fe}$  X-ray source and  $^{90}\text{Sr}/^{90}\text{Y}$  coated  $\beta$  sources of various activities. The activity measurement system is established as a national primary standard for calibration of coated  $\beta$  sources at Radiological Laboratory at BARC. Design and performance of the chamber are presented.

**Keywords.** Surface contamination; windowless proportional counter; beta counting chamber; large area coated sources.

PACS Nos 29.40.Cs; 29.40.n; 87.56.B

### 1. Introduction

Surface contamination monitors used for radiological protection are calibrated using large area  $\beta$  reference sources for detection efficiency of surface emissions. Activity of these sources is not quantitatively determined by the specific activity of the radioactive sample used in source preparation. Considering the effects of self-absorption and back scattering, it is essential to measure the surface emission rate of these sources. As per the international regulations [1] (ISO 1988), calibration of contamination monitor needs a minimum active source area of  $100 \text{ cm}^2$ . Standard laboratories worldwide use gas flow-type large proportional counters to determine absolute surface emission rates from the large-area-coated  $\alpha$ - $\beta$  sources [2–6]. Extended source is introduced directly within the detection volume of the detector to avoid any loss of detection efficiency due to absorption in the entrance window.

A windowless flow-type proportional counter (PC) is developed as per the recommendations for reference transfer instrument [7] (ISO 8769). The detector needs to be highly reliable, user-friendly and rugged with minimum maintenance. A tailor-made detector for the user-specific  $\beta$  sources is designed, developed and characterized for the first time in the country. Performance of the chamber using coated sources shows the length of the plateau to be  $\sim 450$  V and the plateau slope to be  $0.3\%/100$  V. These values are better than the values of other chambers reported in the literature [2,6]. Good stability of operation and repeatability of the results is observed. The detector is installed successfully at BARC and has been established as a national primary standard for calibration of the reference sources.

## **2. Design of the chamber**

PC is based on a multiwire anode grid covering a large sensitive area of the source. The source is directly introduced within the sensitive volume of the MWPC and radiations emitted in near  $2\pi$  solid angle are measured through gas ionization, thus counting losses due to absorption in the entrance window are avoided.

### *2.1 Choice of the fill gas*

The properties of the fill gas suitable for the operation of multiwire chamber are [8–10] high absorption cross-section, Townsend coefficient, drift velocity of ions and diffusion coefficient. Choice of noble gases for the detection is based on specific ionization and absorption cross-section of the gas.

### *2.2 $Sr^{90}$ decay scheme and range of electrons in gas*

In  $Sr^{90}$  beta decay (figure 1a), the nuclear decay energy is shared between the  $\beta$  particle, the recoiling daughter nucleus and an antineutrino. In this situation, the  $\beta$  particles have continuous spectra with energies ranging from 0 up to the maximum possible energy value,  $E = 0.546$  MeV.  $^{90}Sr / ^{90}Y$  source emits low-intensity energies from 0 to 2.25 MeV as shown in figure 1b [11]. Stopping power of  $\beta$ -rays of various energies in Ar and Kr gases is calculated and plotted in figure 2a and it indicates the higher stopping power with Ar gas for the energy of interest. Figure 2b shows the ranges of  $\beta$ -rays of various energies in Ar gas, calculated using NIST standard datasheets [12]. The extrapolated or practical range of electrons,  $R$ , is defined as the thickness of the material at which the extension of the linearly decreasing region of the transmission curve becomes zero [13]. Range of  $\beta$ -rays in Ar gas at STP calculated for energies 0.546, 1 and 2.25 MeV is 10.48, 25.49 and 127.1 mm, respectively.  $\beta$ -rays emitted in sensitive volume are needed to be stopped within the volume. Emission of  $\beta$ -rays from the central region and normal to the source plane has 50 mm path length and those emitted at large angles and nearly parallel to source plane has 150 mm path length. Gas length of 5 cm is chosen, considering attenuation of  $\beta$ -rays in the sensitive volume and electric field distribution for drift of ions. Figure 2a shows the stopping power of Ar and Kr for  $\beta$ -rays of various energies. Considering the range of energy of interest, Ar is chosen as the fill gas for the detector with the quencher  $Ar+CH_4$  at 1.1 bar.

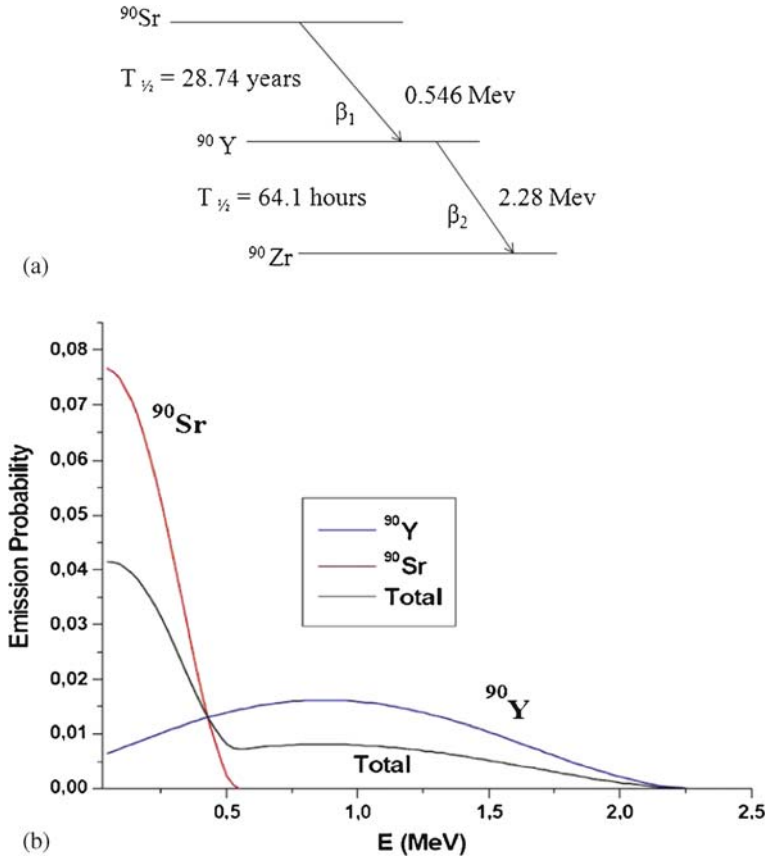


**Figure 1.** (a) Energy levels of  $^{90}\text{Sr}$  decay scheme and (b) energy distribution of  $\beta$ -rays from the  $^{90}\text{Sr}/^{90}\text{Y}$  source.

The detector is designed with a moderate count rate capability of  $\sim 10^4$  CPS for accurate measurements. High voltage is applied to the anode grid and high electric field is generated in the vicinity of each anode wire. The electrostatic field near the surface of the anode wire in the multiwire proportional counter [8–10] is given by

$$E = \frac{V}{(d/2) \left( \left[ (\pi l/s) - \ln(\pi d/s) \right] \right)}, \quad (1)$$

where  $d$  is the diameter of the anode wire,  $s$  is the wire spacing,  $l$  is the anode–cathode gap and  $V$  is the anode voltage. Drift of primary electrons to anode follows the trajectories of field lines from cathode to the anode and high field region is created around  $100 \mu\text{m}$  of the anode, resulting in gas amplification and pulse formation.

### 2.3 Hardware of $2\pi\beta$ proportional counter

The PC consists of a gas enclosure with multiwire grid placed at the centre and a movable sample holder tray. The chamber is made up of aluminum (A16061) and overall dimensions

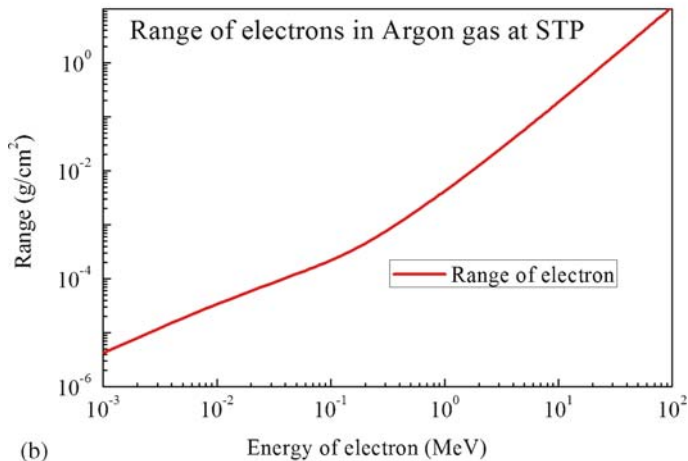
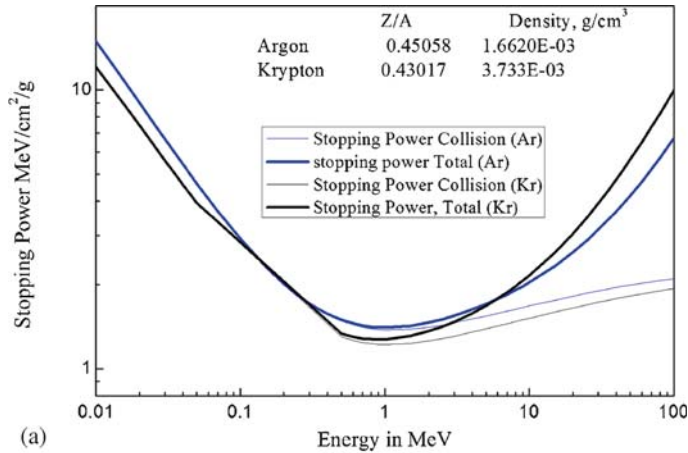


**Figure 2.** (a) Stopping power of Ar and Kr gas and (b) range of  $\beta$ -rays of various energies in Ar gas.

are given in table 1. Sensitive area of the multiwire field grid (20 cm  $\times$  30 cm) is double the size of the source (10 cm  $\times$  15 cm) to cover the emissions  $\sim 2\pi$  solid angle. Detection volume consists of a multiwire anode grid (figure 3a) made up of an array of 25  $\mu$ m Au-plated W wires at the pitch of 20 mm and secured with uniform tension of 0.35 N [8–10]. End wires of the grid mounted with larger diameter for field corrections. All anode wires are bridged at one end and connected through a hermitically sealed connector. Sliding tray consists of a sample holder socket with a slot to secure the source in position. Source sample and anode grid are separated with 25 mm space and total gas length in sensitive volume is 50 mm normal to the plane of the source. Angles of emission from the centre and the edge of the source subtended on anode grid are 165° and 158° along the length of the rectangular source and are 165° and 154° along the breadth of the source.  $\beta$ -rays emitted from the source travel through the path length 50 mm normal to the anode grid

**Table 1.** Specifications of the multiwire β counting chamber.

Description	Dimensions
Overall dimensions	70 cm × 40 cm × 6 cm
Overall weight	8 kg
Sliding tray dimensions	35 cm × 25 cm
Sensitive volume	32 cm × 22 cm × 5 cm
Gas volume at STP	~4 l
Anode grid	Size 30 × 20 cm wires ~25 μm diameter, Au plated W at 20 mm pitch
Vacuum	10 <sup>-3</sup> Torr
Pressure	1.1 ± 0.1 bar
Digital pressure gauge	range 0–20 bar, 0.01 bar accuracy
Flow rate	40–100 cm <sup>3</sup> /min
Fill (flow) gas	P-10 (Ar + 10% CH <sub>4</sub> )
Source	<sup>90</sup> Sr/ <sup>90</sup> Y coated on Al substrate

and 150 mm along the anode grid. Thus, the geometry ensures ~100% absorption of the β-rays emitted within the sensitive region.

PC is hermetically sealed using an O-ring and four latch-type toggle clamps with a pressure tolerance of 15 kg. A suitable provision for frequent manual loading/unloading of the source samples in the source tray is made. Overall machining of the chamber is smoothly polished and is compatible to vacuum of 10<sup>-5</sup> Torr. A digital pressure gauge with an accuracy of 10 mbar and a flow meter for purging of gas are mounted on the chamber. Schematic of the detector construction and complete detection system are shown in figures 3a and 3b respectively. Chamber assembly is shown in figure 4. Chamber is evacuated to high vacuum (10<sup>-5</sup> Torr) and out-gassed at 60°C for 10 days (×24 h) to improve the life of the detector. During regular operation, it is evacuated to 20 mbar and then purged with the fill gas. Gas flow-type detectors though routinely are not evacuated, but it is implemented to reduce the wastage of high-purity gas in purging the large detection volume (~4 l).

### 3. Working of the detector

Completely assembled chamber is initially characterized with the collimated X-ray source <sup>55</sup>Fe to verify hardware perfection and symmetry of the anode–cathode assembly. For this purpose, source holder tray is replaced by a top plate enclosure window having matrix of 12 × 8 equispaced through holes at 20 mm × 20 mm pitch (figure 5a). Top plate is covered with an aluminized Mylar sheet of 10 μm thickness acting as an entrance window for X-ray source. Collimated hole pattern covers the sensitive area (220 mm × 140 mm) of the detector and is suitable to align the source along the wire. This assembly is filled with the Ar+10% CH<sub>4</sub> gas at 1 bar. Pulse height distribution is recorded using a collimated X-ray source <sup>55</sup>Fe by scanning the source over the entire sensitive area, step by step. Peak positions of the pulse height spectra correspond to internal gas amplification factor (~1000) and are plotted across 96 positions on the anode grid. Figure 6 shows the anode

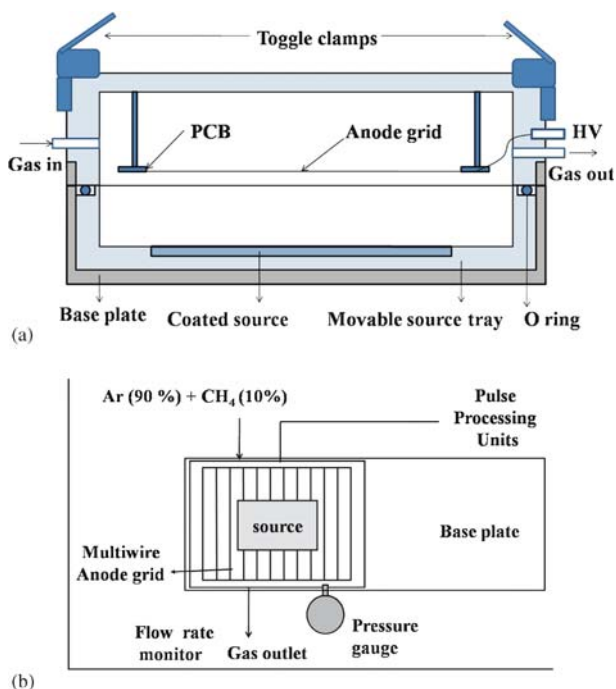


**Figure 3.** Schematic of MWPC. (a) Side section view of the PC structure and (b) PC with accessories.

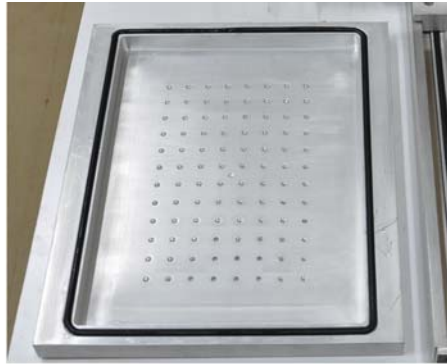
grid lay-out of  $20\text{ cm} \times 30\text{ cm}$  and the typical pulse height distribution at three positions on the anode grid. The top left corner of figure 6 shows the spectra from extreme edge of the grid, where the gas gain is low. Figure at the central part of the grid represents the spectra over the grid area excluding edges of 2 cm and the spectra at the right bottom of the grid show the spectra from source position at 2 cm edges of grid. Figure 7 shows the wire frame profile plot of the pulse height with the position of collimated X-ray source. Plot indicates variation of pulse height and internal amplification over the sensitive area of the anode grid. Uniform gas gain over 80% of the sensitive region indicates geometrical perfection of the anode-cathode assembly of the chamber. Thus, it electronically confirms the absence of any deformity such as dust, kink or sagging of wires. Gas gain is lower at all the edges of the grid and it is expected due to the end effects in electric field distribution. Though gas gain varies over the region, counting efficiency is uniform over 99% of the grid. Pulse height distributions from a collimated  $^{55}\text{Fe}$  source, aligned precisely with one of the anode wires, is shown in figure 8a. Energy resolution is recorded to be  $\sim 18\%$  FWHM at 5.89 keV. Figure 8b shows the pulse height distribution recorded for 1000 s from a  $^{55}\text{Fe}$  source, mounted at a height of 30 cm above the window and the entire sensitive area through the grid holes is illuminated. The broadened peak is the resultant distribution integrated over the grid. Performance of the detector with respect to energy resolution of X-ray peak was consistent after seven days of gas filling, thus indicating the capacity of the detector to hold gas purity and pressure.



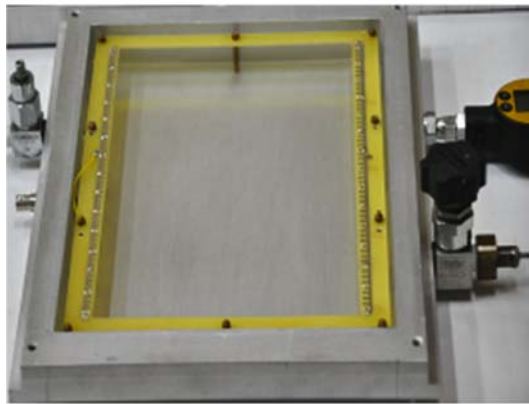
**Figure 4.** Completely assembled  $2\pi$ - $\beta$  chamber in operation with vacuum accessories.

#### **4. Characterization of the chamber using $^{90}\text{Sr}/^{90}\text{Y}$ coated sources**

The chamber is characterized using three large-area  $^{90}\text{Sr}/^{90}\text{Y}$  coated  $\beta$  sources of various strengths. A source is introduced within the detector volume and the detector is filled with Ar + CH<sub>4</sub> gas to a pressure of 1.1 bar and flow rate is adjusted to  $\sim 40$  cm<sup>3</sup>/min. Coated source consists of an array of quantitative drops of sample on aluminum substrate affixed using anodizing process. The source is rectangular with 100 mm  $\times$  150 mm dimension, suitable to fit in the socket provided in the sliding tray. Energy distribution of the  $^{90}\text{Sr}/^{90}\text{Y}$  source has continuum emission spectra of  $\beta$ -rays with a maximum energy of 0.546 MeV from  $^{90}\text{Sr}$  as shown in figure 1b which also shows all the probable energies up to 2.25 MeV from  $^{90}\text{Y}$ . Pulse height distribution resulting from the coated source, shown in figure 9, indicates a peak at 2.0 V pulse height. Higher energy  $\beta$ -rays have  $\sim 120$  mm range in Ar gas. Due to the source grid geometry and the angle of emission,  $\beta$ -rays may not be completely attenuated. Thus, pulses resulting from high-energy emissions result in small pulse amplitude and contribute to the count, if the amplitude is higher than the discrimination voltage level. The sources of various activities used for characterizing the chamber are in the range of 4.5–90 Bq/cm<sup>2</sup> as mentioned in table 2. Total activity of each source ranges from  $7 \times 10^2$  Bq to  $1.5 \times 10^4$  Bq. Details of the sources used to test the



(a)



(b)

**Figure 5.** (a) Enclosure window with collimator holes at  $20\text{ mm} \times 20\text{ mm}$  pitch and covered with aluminized Mylar and (b) top plate with multiwire grid.

detector and average counts recorded are listed in table 2. Pulse height distribution recorded with the source no. 7400 is shown in figure 9. High voltage counting curves are recorded with the coated  $^{90}\text{Sr}/^{90}\text{Y}$  sources of various activities and are shown in figure 10. Plot indicates log scale to cover the range of source strengths in a single plot. Length of the plateaus for all the sources is  $\sim 450\text{ V}$  and the average plateau slope is  $0.3\%/100\text{ V}$ . Good stability of operation and repeatability of the results are observed. Background counts without the source are  $\sim 4\text{ counts/min}$ . The activity of a reference source of the preferred size should be such as to give surface emission rate from  $100$  to  $10000\text{ s}^{-1}$  in order to optimize between background, statistical and dead-time errors. Pulses with smaller pulse heights and being discriminated with the noise, result in the losses. The activity shall be stated with an uncertainty not exceeding  $\pm 3\%$  for the  $\beta$  sources. The average detection efficiency for a given source geometry is  $52.5\%$ . For source no. 7430 with a coated area of  $137.7\text{ cm}^2$  and an activity of  $70\text{ Bq/cm}^2$ , the total emissions estimated in  $2\pi$  solid angle are  $5025\text{ counts/s}$ . The measured average emissions are  $5046\text{ counts/s}$ . For the present source detector geometry, only  $50\%$  of the total emissions from the source are

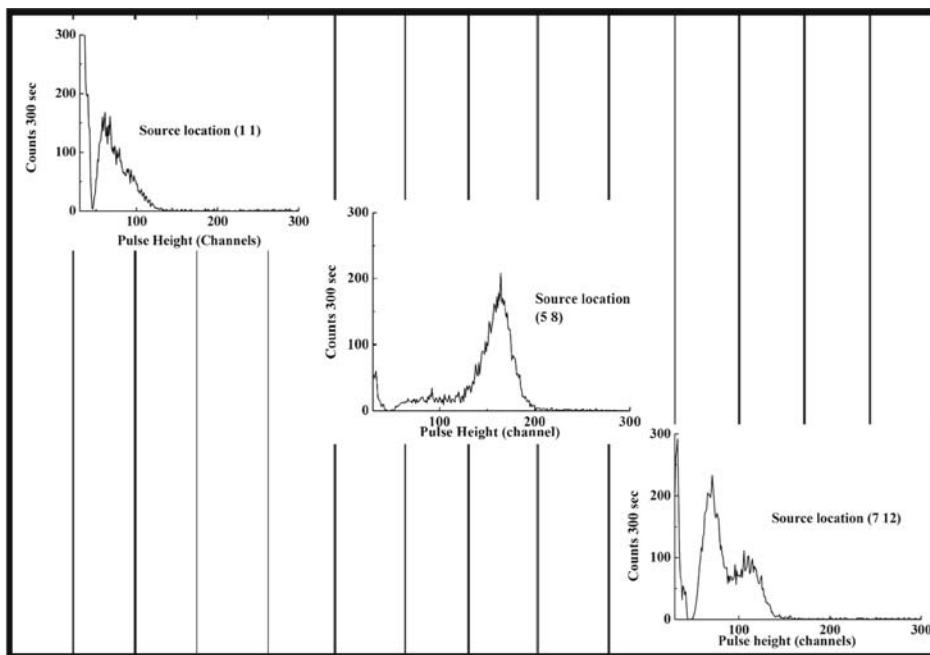


**Figure 6.** Pulse height distributions at various locations on the anode grid.

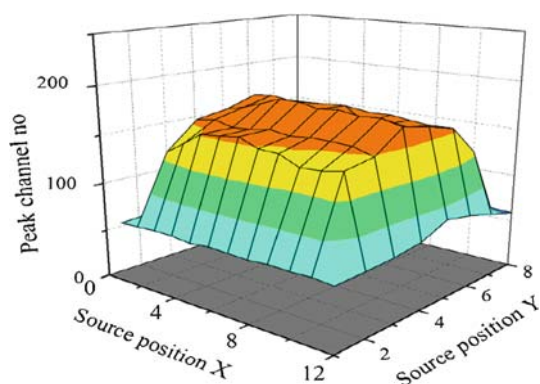


**Figure 7.** Pulse height variation profile over the sensitive region covered by the collimator window.

released in gas volume and are detected. Detection efficiency of the  $\beta$  emissions released in the chamber volume is  $\sim 100\%$ .

The increase in the counts is due to back-scattering from the substrate. The losses in emissions are also anticipated due to self-absorption in the source-coating. These factors are consistent in all the measurements. Correction factor is normalized using the average counting data for all the three sources.  $A = 2kF_b$  [2], where  $A$  is the source activity related to  $\beta$  emission flux  $F_b$  and  $k$  is the correction factor by considering self-absorption and back-scattering. The measured average value of  $k$  for three sources is 0.956. Figure 11

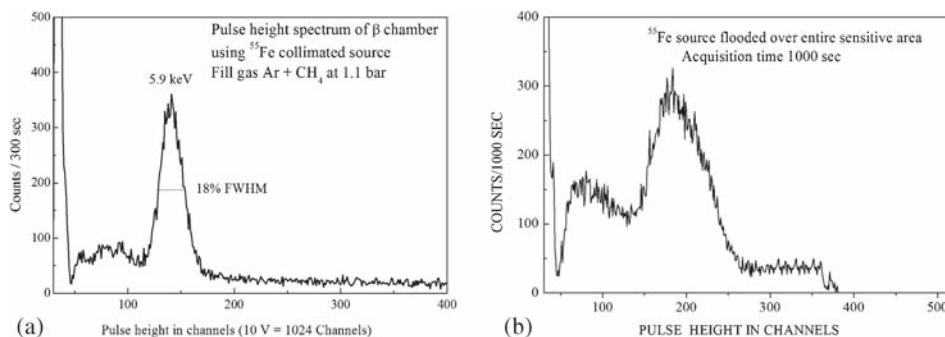


**Figure 8.** Pulse height spectra with  $^{55}\text{Fe}$  source placed at (a) collimator aligned with the anode wire and (b) flooded over the entire sensitive region of the chamber.

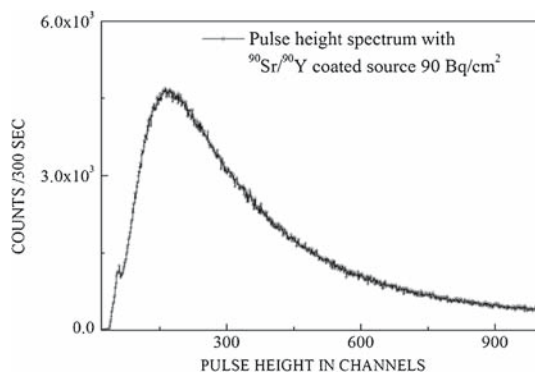


**Figure 9.** Pulse height spectrum of the PC with the  $^{90}\text{Sr}/^{90}\text{Y}$  source no. 7400.

**Table 2.** Specifications of the large-area  $^{90}\text{Sr}/^{90}\text{Y}$  coated  $\beta$  sources.

Label	Source strength (Bq/cm <sup>2</sup> )	Coated area (cm <sup>2</sup> )	Total emission rate	Counts/s	Efficiency (%)
7236	−4.5	15 × 10	675.0	363.5	53.8
7340	−70	14.5 × 9.5	9642	5045.7	52.3
7400	−90	14.5 × 9.5	12393	6379.6	51.4

shows the linearity of emission rate with source activity with an accuracy of 0.99. The maximum activity presently recorded with the PC is 90 Bq/cm<sup>2</sup>. Considering the rise time of the pulse and dead time of the detector, dynamic range for linearity of the total source activity is between 150 Bq and 2 × 10<sup>4</sup> Bq. The source strengths between 1 and 260 Bq/cm<sup>2</sup> are suitable for the given source size. Dead time of the chamber measured using two source methods with X-ray sources is ~20  $\mu\text{s}$ . Further tests with a number of higher and lower activity sources are needed for setting practical limits for dynamic range for calibration of source strengths. Considering the smaller range of  $\alpha$ -particles, the present chamber can be efficiently used for  $\alpha$ -ray emitting sources.

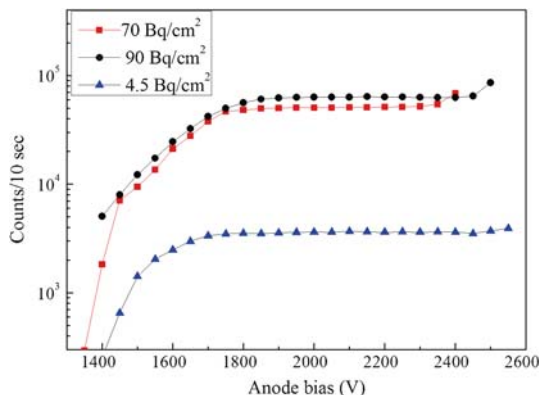


**Figure 10.** Voltage counting curve using the  $^{90}\text{Sr}/^{90}\text{Y}$  coated sources of various activities.

## 5. Results and discussion

A flow-type multiwire detector for calibrating large-area  $\beta$  sources in  $2\pi$ -geometry is successfully developed. Characterization of the MWPC using  $^{90}\text{Sr}/^{90}\text{Y}$  coated sources of known activity was carried out. Counting plateau with anode bias shows a stable plateau length of 450 V and well comparable and in some cases better than the values mentioned in the literature [2–6]. It may be due to the geometric perfection and precautions for maintaining gas purity by introducing additional evacuation stage. Position-dependent tests of the chamber using collimated X-ray source are carried out to record the variation of internal gas gain over the sensitive region. Uniform gas gain over 80% of the sensitive region indicates perfect geometrical symmetry. Uniformity of counting over the source area is 99%. The chamber is installed at the user facility and is operated over a year with good stability, linearity and repeatability of measurements. The chamber is established

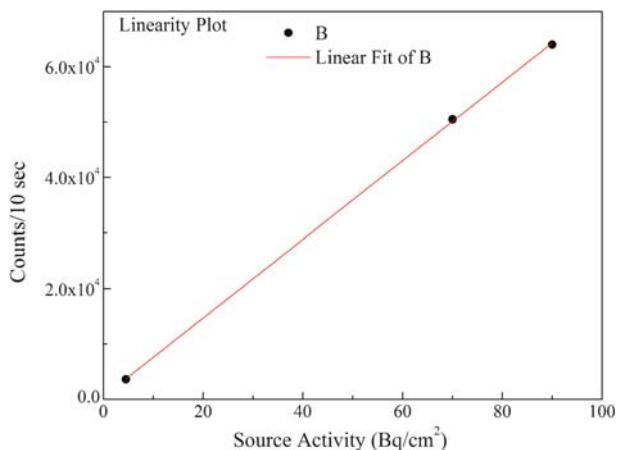


**Figure 11.** Linearity plot of counts vs. source activity.

as the national primary standard for the calibration of large-area reference sources. The present chamber is also suitable for the calibration of  $\alpha$  emitting large area coated sources.

### **Acknowledgements**

The author is thankful to RPAD, BARC for proposing the chamber requirement and making various sources available for the characterization of the chamber. The author would also like to thank MDPDD workshop, BARC for the precise machining of chamber parts. Help of Mrs Shylaja Devan and Shri S M Patkar during the assembly and testing of the chamber is appreciated.

### **References**

- [1] ISO (1988) Reference sources for the calibration of surface contamination monitors – Beta-emitters (maximum beta energy greater than 0.15 MeV) and alpha-emitters, International Organization for Standardization (ISO) 8769 1st Edn, 1988-06-15
- [2] H Janssen and R Klein, *Nucl. Instrum. Methods A* **339**, 318 (1994)
- [3] Jyi-Lan Wu, Ming-Chen Yuan, Shi-Hwa Su and Wen-Son Hwang, *Appl. Radiat. Isot.* **56**, 261 (2002)
- [4] K B Lee, Jong Man Lee and Tae Soon Park, *Appl. Radiat. Isot.* **63**, 99 (2005)
- [5] L E King, J M R Hutchinson and M P Unterweger, *Appl. Radiat. Isot.* **66**, 877 (2008)
- [6] J C Mostert, *Appl. Radiat. Isot.* **66**, 925 (2008)
- [7] ISO 8769 Reference sources – Calibration of surface contamination monitors – Alpha-, beta- and photon emitters, 2nd Edn, 2010-09-01
- [8] G Charpak, R Bouclier, T Bressani, J Favier and C Zupancic, *Nucl. Instrum. Methods* **62**, 262 (1968)
- [9] F Sauli, *Principles of operation of multiwire proportional and drift chambers*, CERN Scientific Report, 77-09 (1977)
- [10] S S Desai, J N Joshi and A M Shaikh, *Pramana – J. Phys.* **59(4)**, 611 (2002)
- [11] Julio Heredia Carmona and Oscar Diaz Rizo, *Experimental and Monte Carlo determination of mass absorption coefficients for  $^{90}\text{Sr}/^{90}\text{Y}$  beta particles in organic compounds*, *Nucleus* [online]. 2009, n.45, pp. 26–31, ISSN 0864-084X
- [12] <http://physics.nist.gov/xcom> (2005)
- [13] *Introduction to health physics*, by Herman Cember, 2nd Edn (Pergamon Press, New York, 1983) p. 97